PAPER

Check for updates

Bifunctional sulfur-rich macrocyclic chelators and their immunoconjugates for the targeted delivery of theranostic mercury-197

Parmissa Randhawa, [ID] [a,b] Misaki Kondo, [ID] [c] Arthur C. K. Chu,[c] Cristina Rodríguez-Rodríguez, [ID] [d,e] Zhongli Cai, [ID] [c] Conrad Chan, [ID] [c] Yumeela Ganga-Sah, [ID] [b] Shaohuang Chen, [ID] [a,b] Neil Weatherall,[b] Patrick R. W. J. Davey, [ID] [a,b] Helen Merkens, [ID] [f] Raymond M. Reilly, [ID] [c] Valery Radchenko [ID] [b,g] and Caterina F. Ramogida [ID] ★[a,b]

The use of chemically matched theranostic radiometals in nuclear medicine presents a paradigm shift in personalized medicine with immense potential to treat advanced cancers. The nuclear isomers, mercury-197g (^{197g}Hg, half-life 64.14 h) and mercury-197m (^{197m}Hg, half-life 23.8 h) possess optimal physical decay properties to be applied in theranostic radiopharmaceuticals; however, their use has been limited due to the lack of suitable bifunctional chelators (BFCs) capable of attaching the radionuclides to disease targeting biomolecules. Herein we report the development and evaluation of two novel $^{197m/g}$Hg BFCs derived from a 15-membered thiacrown ether macrocycle (NS$_4$) bearing isothiocyanate (−NCS) or tetrazine (−Tz) bifunctional handles to allow conjugation to biomolecules. Both chelators were synthesized and radiolabeled with $^{197m/g}$Hg, assessed for complex stability, and bioconjugation to trastuzumab (TmAb), a monoclonal antibody targeting HER2 receptors. **NS$_4$-Tz** efficiently and stably complexes [$^{197m/g}$Hg]Hg^{2+} and exhibited excellent *in vitro* stability in both glutathione and human serum. In contrast, **NS$_4$-NCS** showed lower radiometal incorporation yields and reduced complex stability, likely attributed to non-specific interactions of the isothiocyanate group with Hg^{2+}. **NS$_4$-Tz** was successfully conjugated to transcyclooctene-modified TmAb with favourable chelator-to-antibody ratios and subsequently radiolabeled. Due to non-specific Hg^{2+} binding to TmAb observed during direct labeling, a two-step labeling strategy was employed to improve selectivity. The resulting [$^{197m/g}$Hg]Hg-NS$_4$-Tz-TmAb construct demonstrated specific binding to HER2-positive SK-BR-3 cells *in vitro* and, in the first *in vivo* study of a [$^{197m/g}$Hg]Hg-labeled immunoconjugate, confirmed tumour-specific uptake in a SKOV-3 xenograft mouse model. Biodistribution and SPECT/CT studies of the BFC complex alone, [$^{197m/g}$Hg]Hg-NS$_4$-Tz, revealed high hepatic and splenic accumulation, with some renal uptake possibly due to transchelation or tracer pharmacokinetics. While long-term *in vivo* stability of the radioimmunoconjugate remains a challenge, **NS$_4$-Tz** shows significant promise for applications with faster-clearing vectors such as peptides or small molecules. Future work will focus on improving hydrophilicity and further optimizing chelator design for mercury-based theranostics.

[a]Department of Chemistry, Simon Fraser University, 8888 University Drive, Burnaby, British Columbia, V5A 1S6, Canada. E-mail: cfr@sfu.ca

[b]Life Sciences, TRIUMF, 4004 Wesbrook Mall, Vancouver, British Columbia, V6T 2A3, Canada

[c]Leslie Dan Faculty of Pharmacy, University of Toronto, 144 College Street, Toronto, Ontario, M5S 3M2, Canada

[d]Faculty of Pharmaceutical Sciences, University of British Columbia, 2405 Wesbrook Mall, Vancouver, British Columbia, V6T 1Z3, Canada

[e]Department of Physics and Astronomy, University of British Columbia, 6224 Agronomy Road, Vancouver, British Columbia, V6T 1Z1, Canada

[f]Department of Molecular Oncology, BC Cancer Research Institute, Vancouver, BC, V5Z 1L3, Canada

[g]Department of Chemistry, University of British Columbia, 2036 Main Mall, Vancouver, British Columbia, V6T 1Z1, Canada

Introduction

The theranostic radionuclide pair mercury-197m and mercury-197g ($^{197m/g}$Hg, $t_{1/2}$ = 23.8 h and 64.14 h, respectively) are promising candidates for Meitner-Auger electron (MAE)-based radioimmunotherapy. Their favourable decay characteristics – long half-lives, high average yields of MAEs per decay (^{197m}Hg: 19.4 and ^{197g}Hg 23.2), and substantial average energies (7.6 and 7.4 keV, respectively) – make them attractive for targeted therapeutic applications.[1–4] However, their use in nuclear medicine has been limited due to the lack of suitable bifunctional chelators (BFCs) capable of stably incorporating

$[^{197m/g}Hg]Hg^{2+}$ into radiopharmaceuticals. A BFC is a critical component of a metal-based radiopharmaceutical, providing robust chemical linkage between the radiometal and the targeting vector while maintaining complex stability and inertness *in vivo*. Traditional commercially available BFCs are unsuitable for $[^{197m/g}Hg]Hg^{2+}$ due to mismatched coordination chemistry, as predicted by Pearson's Hard–Soft-Acid–Base (HSAB) theory.[5–9] To address this gap, our group has developed thioether-based macrocyclic ligands with selective affinity for $[^{197m/g}Hg]Hg^{2+}$ that form kinetically inert complexes.[10] In particular, the *N*-benzyl-2-(1,4,7,10-tetrathia-13-azacyclopentadecan-13-yl)acetamide (**NS$_4$-BA**) (Fig. 1) demonstrated excellent complexation with $[^{197m/g}Hg]Hg^{2+}$ at both 80 °C and 37 °C within 60 minutes at 10^{-4} M ligand concentration. The resulting complexes remained inert *in vitro* when challenged with human serum and glutathione.[10] Despite this promising performance, **NS$_4$-BA** lacks a functional group for conjugation to biomolecules, preventing its use in targeted delivery approaches.

To address this limitation, we designed and synthesized two novel BFCs based on the **NS$_4$-BA** scaffold: an isothiocyanate-functionalized derivative (**NS$_4$-NCS**) and a tetrazine-functionalized derivative (**NS$_4$-Tz**), as shown in Fig. 1. These BFCs were designed for conjugation to the HER2-targeting monoclonal antibody Trastuzumab (TmAb, marketed as Herceptin)[11–13] to enable proof-of-concept targeted preclinical *in vivo* studies.

Given the wide variety of available functional groups for antibody conjugation, we focused on two clinically relevant strategies. The –NCS group was chosen for its ability to directly and covalently bind to lysine residues on antibodies. Additionally, we incorporated a tetrazine (–Tz) moiety to enable biorthogonal "click" chemistry, specifically the fast Inverse Electron Demand Diels–Alder (IEDDA) reaction with *trans*-cyclooctene (TCO, $k \sim 1 \times 10^6$ M^{-1} s^{-1}).[14] This reaction allows for pretargeting strategies that mitigate radiation to healthy tissue, a limitation in current radioimmunotherapy due to prolonged circulation of radiolabeled antibodies.[15–18] In the pretargeting approach, the slowly-localizing TCO-modified antibody is administered and allowed to localise

first before the Tz-modified radiotracer is administered, improving the therapeutic index and enabling individualized treatment.[17,19,20]

Herein, we report the synthesis of **NS$_4$-NCS** and **NS$_4$-Tz**, evaluate their ability to chelate $[^{197m/g}Hg]Hg^{2+}$, and assess the *in vitro* and *in vivo* stability of the resulting complexes. We also demonstrate their conjugation to TmAb, radiolabeling of the immunoconjugates, and performance in targeted *in vitro* cell binding assays. Finally, we present the first preclinical *in vivo* study of targeted delivery using a $[^{197m/g}Hg]Hg^{2+}$-labeled radioimmunoconjugate, highlighting both the promise and the potential challenges of this approach for future theranostic applications.

Experimental

Materials and methods

All solvents and reagents were purchased from commercial suppliers and used as received unless otherwise noted. Ultrapure concentrated hydrochloric acid (HCl, 99.99% trace metal grade, 37%), sodium hydroxide (NaOH, ACS reagent, ≥97%, pellets), octanol, dimethyl sulfoxide (DMSO), L-glutathione, 4-(Boc-amino)benzylamine and human serum were purchased from Sigma Aldrich (St Louis, MO) and used as received. Tetrazine amine HCl ((4-(1,2,4,5-tetrazin-3-yl)phenyl)methanamine), methyltetrazine HCl ((4-(6-methyl-1,2,4,5-tetrazin-3-yl)phenyl)methanamine), and TCO-PEG$_4$-NHS ester were purchased from Click Chemistry Tools (Newmark, CA) and used as received. Phosphate Buffered Saline (PBS) was purchased from Cytiva (Vancouver, BC). 20× PBS Tween-20 buffer was purchased from Thermo Fisher Scientific Inc. (Waltham, MA) and diluted with ultrapure water to 1×. Millipore system (Direct-Q® 3UV with Pump, 18 MΩ cm^{-1}) provided ultrapure water. Deuterated solvents used for NMR analysis were purchased from Sigma or Cambridge Isotope Laboratories Inc. (Tewksbury, MA) and exhibited an isotopic purity between 99.9% and 99.8%. Solvents noted as "dry" were obtained following storage over 3 Å molecular sieves under an argon environment. All NMR spectra were recorded on a Bruker AVANCE III 600 MHz QCI cryoprobe, Bruker AVANCE III 500 MHz, or Bruker AVANCE III 400 MHz instruments. Chemical shifts are reported in parts per million (ppm) and are referred to as the residual solvent peak. Multiplicity is reported as follows: s = singlet, t = triplet, m = multiplet, and br = broad peak. The coupling constants (J) are reported in hertz (Hz). High-resolution electrospray-ionization mass spectrometry (ESI-HRMS) was performed on an Agilent 6210 time-of-flight (TOF) instrument using a Halo LC-MS column (5 μm, C18, 90 Å, 2.1 × 50 mm) (solvent system – A: 90% H$_2$O, 10% MeCN, 6 mM NH$_4$OAc; B: 10% H$_2$O, 90% MeCN, 6 mM NH$_4$OAc; gradient: 0% B (0–0.5 min), 0–100% B (0.5–6.0 min), 100% B (6.0–6.7 min), 100–0% B (6.7–6.8 min), 0% B (6.8–8 min); flow rate: 0.4 mL min^{-1}. Semi-preparative high-performance liquid chromatography (HPLC) was performed using an Agilent Technologies 1100 system equipped
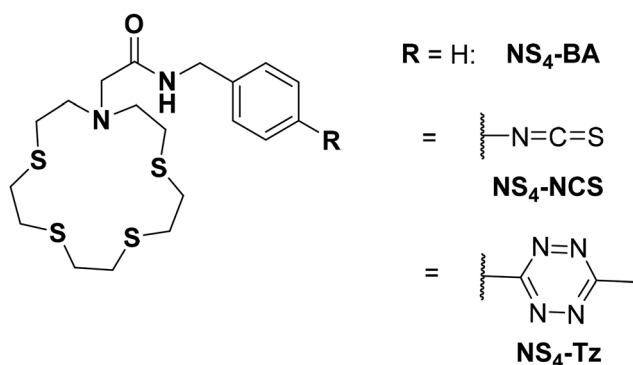

Fig. 1 The previously studied **NS$_4$-BA** and novel NS$_4$-derived bifunctional chelators, **NS$_4$-NCS** and **NS$_4$-Tz**, developed within.

with a quaternary pump, UV-vis detector monitoring at 254 nm, Phenomenex Luna column (5 μm, C18, 100 Å, 150 × 10 mm), and fraction collector was used for the analysis and semi-prep purification. The radiolabeling of ligands was monitored using silica-impregnated instant thin-layer chromatography paper (iTLC-SG, Agilent Technologies, Santa Clara, CA, USA). Data were analyzed on an Eckert & Ziegler AR-2000 TLC scanner and processed with Eckert & Ziegler WinScan software (Hopkinton, USA). A Capintec CRC-55tR dose calibrator set at the ^{197g}Hg calibration (calibration number: 197) was used to measure the radioactive sample and measurements were cross-referenced with the gamma spectrometer value to ensure accuracy in the reading values. The Capintec was used to measure the activity before radiolabeling reactions. Bio-rad Mini-PROTEAN Tetra Vertical Electrophoresis Cell instrument was used for all Sodium Dodecyl Sulphate – PolyAcrylamide Gel Electrophoresis (SDS-PAGE) measurements with 4–20% Mini-PROTEAN® TGX™ Precast Protein Gels. The SDS-PAGE gel electrophoresis reagents, including the MW standards, TGS buffer, Laemmli sample buffer, and Bio-SafeTM Coomassie stain, were also purchased from Bio-rad. Trastuzumab was purchased as Herceptin from Genentech and purified using an SEC column (PD-10 or Minitrap, Sephadex G-25 resin, Cytiva) followed by spin filtration using a 50 000 molecular weight cut-off filter (Amicon Ultra-0.5 centrifugal units, Ultracel 50: regenerated cellulose, Millipore). The antibody solution in PBS (pH 7.4) was stored at 4 °C for 6 months. Following previously reported procedures, MALDI-ToF MS/MS determined the average number of TCO or moieties per antibody on a Bruker autoflex speed at the Alberta Proteomics and Mass Spectrometry Facility (University of Alberta, Canada).[21] The [M + 2H]$^{2+}$ mass signals were used to determine the average mass and calculate the antibody-to-TCO and antibody-to-chelate ratios. UV-vis measurements to determine the concentration of the antibody solutions were performed on a Thermo Scientific NanoDropTM 1000 using the antibody (~150 kDa) extinction coefficient of 210 000 M^{-1} cm^{-1}.

Caution!!! [$^{197m/g}$Hg]Hg^{2+} produces ionizing radiation and should be handled in laboratories approved for radioactive work using safe lab practices. All work with radionuclides was undertaken in shielded fume hoods to minimize dose to experimenters (and special precautions were used to prevent contamination) under nuclear energy worker (NEW) status earned by attending TRIUMF's Advanced Radiation Protection course and passing the final exam.

Caution!!! Mercury is a toxic heavy metal, and its compounds should be treated accordingly.

Synthesis and characterization of NS$_4$ BFC derivatives

The 2-(1,4,7,10-tetrathia-13-azacyclopentadecan-13-yl)acetic acid (NS$_4$-CA) was prepared using the previously published procedure from Randhawa *et al.*[10]

2-(1,4,7,10-Tetrathia-13-azacyclopentadecan-13-yl)-*N*-(4-(6-methyl-1,2,4,5-tetrazine-3-yl)benzyl)acetamide (NS$_4$-Tz). To a solution of NS$_4$-CA (25.3 mg, 0.074 mmol, 1 eq.), DIPEA (55 μL, 0.3145 mmol, 4.2 eq.) and HATU (55.7 mg, 0.146 mmol, 2 eq.)

in dry DMF (10 mL), methyltetrazine–amine HCl (18.7 mg, 0.093 mmol, 1.2 eq.) was added. The reaction mixture was covered in foil and left at room temperature overnight under argon. After completion of the reaction (monitored *via* MS), the mixture was evaporated under vacuum, then washed with water and saturated sodium bicarbonate (2 × 10 mL each) and extracted using ethyl acetate (3 × 10 mL). Organic phases were collected and dried over Na$_2$SO$_4$. After filtration, volatiles were removed under vacuum to yield a bright pink solid. The recovered solid was further purified by reverse-phase semipreparative high-performance liquid chromatography at 4.5 mL min^{-1} with the following method: A: H$_2$O with 0.1% formic acid (FA), B: acetonitrile (CH$_3$CN) with 0.1% FA; 0–0.5 min 0% B; 0.5–10 min 0–100% B, 10–11 min 100% B. The fraction at 8.51 min was collected and lyophilized to yield **NS$_4$-Tz** (29.8 mg, 77% yield) as a pink solid. ESI-HRMS *m/z* calcd for [C$_{22}$H$_{32}$N$_6$OS$_4$ + H]$^+$ 525.160; found 525.159 [M + H]$^+$. ^{1}H NMR (600 MHz, CDCl$_3$) δ 8.60 (d, *J* = 8.1 Hz, 2H), 8.19 (t, *J* = 6.1 Hz, 1H), 7.58 (d, *J* = 8.0 Hz, 2H), 4.62 (d, *J* = 6.1 Hz, 2H), 3.24 (s, 2H), 3.12 (s, 3H), 2.83–2.67 (m, 20H). ^{13}C NMR (151 MHz, CDCl$_3$) δ 171.05, 167.40, 163.98, 143.40, 131.05, 128.95, 128.35, 58.91, 54.97, 43.02, 33.43, 32.67, 32.25, 31.10, 21.33.

***N*-(4-(1,2,4,5-Tetrazin-3-yl)benzyl)-2-(1,4,7,10-tetrathia-13-azacyclopentadecan-13-yl)acetamide (NS$_4$-Tz-H).** To a solution of NS$_4$-CA (5.0 mg, 0.0146 mmol, 1 eq.), DIPEA (10.2 μL, 0.059 mmol, 4 eq.) and HATU (8.3 mg, 0.021 mmol, 1.5 eq.) in dry DMF (20 mL), tetrazine-amine HCl (3.3 mg, 0.018 mmol, 1.2 eq.) was added. The reaction mixture was covered in foil and left at room temperature overnight under argon. After completion of the reaction (monitored *via* MS), the mixture was evaporated under vacuum, then washed with water and saturated sodium bicarbonate (2 × 10 mL each) and extracted using ethyl acetate (3 × 10 mL). Organic phases were collected and dried over Na$_2$SO$_4$. After filtration, volatiles were removed under vacuum to yield a bright pink solid. The recovered solid was further purified by reverse-phase semipreparative high-performance liquid chromatography at 4.5 mL min^{-1} with the following method: A: H$_2$O with 0.1% formic acid (FA), B: acetonitrile (CH$_3$CN) with 0.1% FA; 0–0.5 min 0% B; 0.5–10 min 0–100% B, 10–11 min 100% B. The fraction at 9.4 min was collected and lyophilized to yield **NS$_4$-Tz-H** (2.9 mg, 39% yield) as a pink solid. ESI-HRMS *m/z* calcd for [C$_{21}$H$_{30}$N$_6$OS$_4$ + H]$^+$ 511.144; found 511.153 [M + H]$^+$. ^{1}H NMR (600 MHz, CD$_3$CN) δ 10.28 (s, 1H), 8.54 (d, 2H), 7.73 (s, 1H), 7.58 (d, 2H), 4.56 (d, *J* = 6.1 Hz, 2H), 3.92 (s, 2H), 3.41 (t, *J* = 7.4 Hz, 4H), 2.93 (t, *J* = 8.2, 6.6 Hz, 4H), 2.91–2.69 (m, 12H). ^{13}C NMR (151 MHz, CD$_3$CN) δ 158.04, 128.51, 128.15, 54.61, 42.59, 32.41, 31.81, 31.54, 27.58 (the 4 tertiary carbons in the molecule could not be seen in the ^{13}C NMR, HSQC or HMBC).

***N*-(4-Aminobenzyl)-2-(1,4,7,10-tetrathia-13-azacyclopentadecan-13-yl)acetamide (NS$_4$-NH$_2$).** To a solution of NS$_4$-CA (80.0 mg, 0.232 mmol, 1 eq.), DIPEA (263.2 μL, 0.937 mmol, 4 eq.) and HATU (133.6 mg, 0.351 mmol, 1.5 eq.) in dry DMF (10 mL), 4-(Boc-amino)benzylamine (62.4 mg, 0.281 mmol, 1.2 eq.) was added. The reaction mixture was left at room temperature overnight under argon. After completion of the reaction

(monitored *via* MS), the mixture was evaporated under vacuum, then washed with water and saturated sodium bicarbonate (2 × 10 mL each) and extracted using ethyl acetate (3 × 10 mL). Organic phases were collected and dried over Na_2SO_4. After filtration, volatiles were removed under vacuum to yield an orange oil. The recovered oil was further purified by reverse-phase semipreparative high-performance liquid chromatography at 4.5 mL min^{-1} with the following method: A: H_2O with 0.1% FA, B: acetonitrile (CH_3CN) with 0.1% FA; 0–0.5 min 0% B; 0.5–10 min 0–100% B, 10–11 min 100% B. The fraction at 9.20 min was collected to which 12 M HCl was added to give a final concentration of ~4 M HCl (2 ml) and lyophilized to yield **NS$_4$-NH$_2$**·HCl (60.4 mg, 54% yield) as a white solid. ESI-HRMS *m/z* calcd for $[C_{19}H_{32}N_3OS_4\text{-Cl}]^+$ 446.143; found 446.152 [M-Cl]$^+$. ^{1}H NMR (600 MHz, MeOD) δ 7.54 (d, J = 8.4 Hz, 2H), 7.41 (d, J = 8.4 Hz, 2H), 4.53 (s, 2H), 4.20 (s, 2H), 3.58 (broad s, 4H), 3.04 (t, J = 7.9 Hz, 4H), 2.94–2.81 (m, 12H). ^{13}C NMR (151 MHz, MeOD) δ 164.23, 139.41, 129.66, 129.14, 122.99, 55.04, 53.89, 42.22, 32.26, 31.71, 31.64, 25.29.

2-(1,4,7,10-Tetrathia-13-azacyclopentadecan-13-yl)-*N*-(4-iso-thiocyanatobenzyl)acetamide (NS$_4$-NCS). To a solution of **NS$_4$-NH$_2$** (7.6 mg, 0.0139 mmol, 1 eq.) in dry CH_2Cl_2 (1.5 mL) and 3 Å molecular sieves (10% *m/v*), triethylamine (20 μL, 0.139 mmol, 10 eq.) was added. The reaction mixture was stirred at room temperature for 15 min then cooled to 0 °C and carbon disulfide (10 μL, 0.139 mmol, 10 eq.) was added. After 15 min, acetyl chloride (3 μL, 0.042 mmol, 3 eq.) was added. The ice bath was removed and stirring was continued for a further 15 min. The reaction was then filtered, the solvent was removed under reduced pressure and was further purified by reverse-phase semipreparative high-performance liquid chromatography at 4.5 mL min^{-1} with the following method: A: H_2O with 0.1% FA, B: acetonitrile (CH_3CN) with 0.1% FA; 0–0.5 min 0% B; 0.5–10 min 0–100% B, 10–11 min 100% B. The fraction at 7.03 min was collected and lyophilized to yield **NS$_4$-NCS** (3.1 mg, 46% yield) as a white solid. ESI-HRMS *m/z* calcd for $[C_{20}H_{29}N_3OS_5 + H]^+$ 488.099; found 488.152 [M + H]$^+$. ^{1}H NMR (400 MHz, CDCl$_3$) δ 7.50 (d, J = 8.1 Hz, 2H), 7.31 (d, J = 7.8 Hz, 2H), 4.45 (d, J = 5.8 Hz, 2H), 3.24 (s, 2H), 2.91–2.55 (m, 20H). ^{13}C NMR (151 MHz, DMSO-d$_6$) δ 170.14*, 138.00*, 133.88*, 127.58, 118.85, 58.01, 54.51**, 42.12, 31.85, 31.41, 28.63, 28.49. *Identified by HMBC **Identified by HSQC (the carbon associated with the isothiocyanate could not be seen in the ^{13}C NMR, HSQC or HMBC).

Trastuzumab bioconjugate synthesis

TmAb-TCO modification. The conjugation reaction closely followed previously reported procedures.[21] The pH of a solution of purified trastuzumab (500 μL, 28.03 mg mL^{-1}, 1 eq.) in PBS (pH 7.4) was adjusted to 8.8–9 by the addition of small aliquots of a solution of 0.1 M Na_2CO_3 (9 μL). TCO-PEG$_4$-NHS ester (9.6 μL, 40 mg mL^{-1}, 8 eq.) in dimethylformamide was added slowly with agitation to the antibody solution. The reaction was incubated at 25 °C in a thermoshaker at 500 rpm for 1 h. The resulting solution was purified by SEC (Minitrap, Sephadex G-25 resin, Cytiva) and the purified Trastuzumab-

PEG$_4$-TCO was collected in PBS (pH 7.4, 3.5 mL). The sample was concentrated by spin filtration (Amicon ultra-0.5, 50k) at 14 000*g* for 5 min and the solution was transferred to a 1.5 mL Eppendorf tube. The filter was washed with 0.2 mL of PBS (pH 7.4) and combined with the modified antibody solution (167.4 μL, 95.83 mg mL^{-1}). The number of TCO units per antibody was found to be 4.08 ± 0.47 (*n* = 3) by MALDI-ToF MS/MS.

NS$_4$-Tz-TmAb *in vitro* click reaction. To a solution of TmAb-PEG$_4$-TCO (TmAb-TCO, as prepared above) (47 μL, 95.8 mg mL^{-1}, 1 eq.) diluted with 1054 μL of PBS (pH 7.4) and 241 μL of DMSO, a solution of **NS$_4$-Tz** in DMSO (90 μL, 10^{-2} M, 30 eq.) was added slowly (2 μL s^{-1}). The resulting solution was sonicated for 1 min and incubated at 25 °C in a thermoshaker at 500 rpm for 1 h. Purification to remove unclicked chelator was carried out by spin filtration (Amicon ultra-0.5, 50k) at 14 000*g* for 5 min. The filter was washed with 0.4 mL of water (0.1% DMSO) (×6) and 0.4 mL of PBS (pH 7.4) (×2) and combined with the clicked antibody solution (120 μL, 16.50 mg mL^{-1}). The ratio of molecules of chelates per modified antibody was 3.0 by MALDI-ToF MS/MS. *Although plenty of reactions were performed varying in their antibody concentration, DMSO concentration and antibody-to-ligand ratio, for click optimization (see Table S1 for more details) these were the conditions which were used for the conjugate in further one-step radiolabeling experiments.

NS$_4$-NCS-TmAb modification. The conjugation reaction closely followed previously reported procedures.[22] The pH of a solution of purified trastuzumab (94.5 μL, 5.29 mg mL^{-1}) in PBS (pH 7.4) was diluted in 142.7 μL of PBS (pH 8.5/9, adjusted with 0.1 M Na_2CO_3). **NS$_4$-NCS** (12.8 μL, 0.01 mol L^{-1}, 40 eq.) in DMSO was added slowly with agitation to the antibody solution. The reaction was incubated at 25 °C in a thermoshaker at 500 rpm for 1.5 h. The resulting solution was purified by SEC (Minitrap, Sephadex G-25 resin, Cytiva) and the purified NS$_4$-NCS-TmAb was collected in PBS (pH 7.4, 3.5 mL). The sample was concentrated by spin filtration (Amicon ultra-0.5, 50 k) at 14 000*g* for 15 min and the solution was transferred to a 1.5 mL Eppendorf tube. The filter was washed with 0.2 mL of PBS (pH 7.4) and combined with the modified antibody solution (130 μL, 1.70 mg mL^{-1}). The number of **NS$_4$-NCS** units per antibody was found to be 1.1 by MALDI-ToF MS/MS.

Production of mercury-197m/g

Production of $[^{197m/g}\text{Hg}]\text{Hg}^{2+}$ was achieved through proton irradiation of natural gold (Au) targets *via* the ^{197}Au(p, n)$^{197m/g}$Hg nuclear reaction at the TR13 (13 MeV) cyclotron at TRIUMF – Canada's particle accelerator center, following previously published procedures, with calculated rate of productions of 4 MBq μA^{-1} h^{-1} for ^{197m}Hg and 2.9 MBq μA^{-1} h^{-1} for ^{197g}Hg.[23] Briefly, Au targets were prepared by the addition of 200–270 mg of Au beads to a 10 mm diameter indent (0.25 mm deep) of a tantalum backing (1 mm in thickness) and melted thereon in a furnace at 1250 °C (Rd-G – RD Webb Company – Natick MA, USA). Following proton irradiation (4 h, 30 μA), the Au target was dissolved in *aqua regia* (3 mL), and the solution was then loaded onto a prepared column of LN

resin (5 g, 25 mL reservoir). $^{197m/g}Hg^{2+}$ was eluted in 6 M HCl (4 mL) while the ^{197}Au was retained on the resin. The $^{197m/g}Hg^{2+}$ solution matrix was then exchanged to a 0.1 M HCl solution by multiple steps of evaporation and reconstitution. The final activity ranged from 90 to 140 MBq of $^{197m/g}Hg^{2+}$ obtained as $HgCl_2$ in 250–350 μL 0.1 M HCl. The radionuclide purity was evaluated using gamma (γ)-ray spectroscopy on an N-type co-axial high-purity germanium (HPGe) gamma spectrometer (CANBERRA, Mirion Technologies, Inc., San Ramon, CA, USA), calibrated with a 20 mL ^{152}Eu and ^{133}Ba source. Samples were prepared by mixing aliquots of $^{197m/g}Hg^{2+}$ activity (1.2 MBq) with deionized water in a 20 mL glass vial to make a 20 mL sample and measured at a distance of 150 mm from the detector for 10 min, ensuring dead times were below 10%. Spectra were analyzed using Genie-2000 software, using the 133.98 keV (I_γ = 33.5%) and 164.97 keV (I_γ = 0.2618%) γ-lines of ^{197m}Hg, and the 77.35 keV (I_γ = 18.7%) γ-line of ^{197g}Hg for activity calculations.[24] The radionuclidic purity was >99%.

$[^{197m/g}Hg]Hg^{2+}$ radiolabeling studies of bifunctional chelators

The **NS₄-Tz** and **NS₄-NCS** ligands were made up as stock solutions (10^{-3} M) in DMSO. A serial dilution was used to prepare ligand solutions at 10^{-4}, 10^{-5} M, 10^{-6} M, and 10^{-7} M in DMSO. An aliquot (10 μL) of each ligand solution (or DMSO, for negative controls) was diluted with ammonium acetate buffer (1 M; pH 7) such that the final reaction volume was 100 μL. $[^{197m/g}Hg]HgCl_2$ (1–1.2 MBq, 3–10 μL) was added and mixed gently to begin the radiolabeling reaction at 37 °C. Complex formation was monitored for each reaction by acquiring the non-isolated percentage radiochemical yield (%RCY) at 1 h. This was achieved firstly by quenching the reaction by extracting an aliquot (10 μL) of the reaction solution and adding it to an equal volume of dimercaptosuccinic acid (DMSA) solution (50 mM, pH 5, 10 μL). The quenched solution was gently mixed and analyzed by spotting a portion (10 μL) of the mixture onto the bottom of an iTLC-SG plate (1 cm × 10 cm, baseline at 1 cm) and then developed using DMSA solution (50 mM, pH 5) as the mobile phase. Under these conditions, the $[^{197m}Hg]Hg^{2+}$-complexes remain at the baseline (R_f = 0), while the unchelated, 'free' $^{197m/g}Hg^{2+}$ migrates towards the solvent front (R_f = 1). TLC plates were analyzed on an Eckert & Ziegler AR-2000 TLC scanner and processed with Eckert & Ziegler WinScan software. Radiolabeling yields were calculated by integrating the peaks in the radio-chromatogram.

$[^{197m/g}Hg]Hg^{2+}$ radiolabeling studies of NS₄-Tz-TmAb

$[^{197m/g}Hg]Hg$-NS₄-Tz-TmAb (1-step labeling). To a solution of 8.9 μL of NS₄-Tz-TmAb in PBS (150 μg) and 97.6 μL of 1 M NH_4OAc pH 7, 3.5 μL of $[^{197m/g}Hg]HgCl_2$ (1.06 MBq) and 3 μL of 6 M NaOH was added simultaneously. The reaction was incubated at 37 °C for 60 min. After confirming reaction completion by iTLC (*via* methods mentioned above), the $[^{197m/g}Hg]$Hg-NS₄-Tz-TmAb was purified by spin filtration (Amicon ultra-0.5, 50 k) at 14 000*g* for 5 min. The filter was washed with 0.4 mL of PBS (pH 7.4) (×6). The labeled tracer was collected in 26 μL, resulting in 0.5 MBq and 86.3 μg of modified TmAb.

$[^{197m/g}Hg]Hg$-NS₄-Tz-TmAb (2-step labeling). To a solution of 50 μL of **NS₄-Tz** in DMSO (10^{-3} M, 20 eq.) and 100 μL of 1 M NH_4OAc pH 7, 20 μL of $[^{197m/g}Hg]HgCl_2$ (12.6 MBq) and 12 μL of 6 M NaOH was added simultaneously. The reaction was incubated at 37 °C for 60 min, and completion was confirmed by iTLC (*via* methods mentioned above). To the $[^{197m/g}Hg]$Hg-NS₄-Tz reaction 4.9 μL of TmAb-PEG₄-TCO (TmAb-TCO, 1 eq.) (91.7 mg mL⁻¹) was added slowly (2 μL s⁻¹). The resulting solution was sonicated for 1 min and incubated at 25 °C in a thermoshaker at 500 rpm for 1 h. Purification to remove unclicked chelate was carried out by spin filtration (Amicon ultra-0.5, 50 k) at 14 000*g* for 5 min. The filter was washed with 0.4 mL of PBS (pH 7.4) (×6). The labeled tracer was collected in 34 μL, resulting in 4.75 MBq and 75.0 μg of modified TmAb. *20 eq. of the 10^{-3} M chelator solution was used rather than the 30 eq. of the 10^{-2} M chelator solution above as MALDI results (Table S1) demonstrated similar chelator per TmAb results of 3.2. Additionally, the solution of lower chelator concentration was easier to handle as fewer of the chelators appeared to precipitate out over the 1 h reaction period.

Glutathione (GSH) competition assay of bifunctional chelators and $[^{197m/g}Hg]Hg$-NS₄-Tz-TmAb

GSH competition assay procedures closely followed those previously developed by our group.[10] To the $[^{197m/g}Hg]$Hg-NS₄-Tz, $[^{197m/g}Hg]$Hg-NS₄-NCS (prepared as described above), radiolabeling controls (DMSO instead of the ligand) or $[^{197m/g}Hg]$Hg-NS₄-Tz-TmAb (prepared as described in the 2-step labeling method above) 50 mM of an L-glutathione (GSH) solution (1 : 22 v/v GSH : reaction solution dilution) was added, and the mixtures were incubated at 37 °C over 137 h or 72 h. The final GSH concentration was chosen to mimic *in vivo* conditions within cells (2.12 mM).[25] The proportion of intact radiolabeled complex was monitored over the course of 137 h or 72 h using iTLC-SG and L-glutathione (50 mM) as the mobile phase. Under these conditions, uncomplexed $^{197m/g}Hg^{2+}$ resulting from GSH transchelation traveled to the solvent front (R_f = 1) while intact $[^{197m/g}Hg]Hg^{2+}$-complex remained at the baseline (R_f = 0).

Human serum stability assay of bifunctional chelators

To the $[^{197m/g}Hg]$Hg-NS₄-Tz and $[^{197m/g}Hg]$Hg-NS₄-NCS (prepared as described above) or radiolabeling controls (DMSO instead of the ligand) was diluted in human serum (1 : 1 *v/v* dilution), and the solutions were incubated at 37 °C over 137 h. The metal-complex stabilities were monitored over 137 h using SDS-PAGE. At each time point, an aliquot (10 μL) of the reaction mixture was mixed with Laemmli sample buffer (10 μL) and was directly loaded onto the SDS-PAGE gel. The SDS-PAGE was run at ambient temperature and 150 V until the dye front reached the resolving gel (1 h). Following electrophoresis, the gel was scanned with the radio-TLC scanner to determine the percentage of the intact complex. The same protocol was used with free $[^{197m/g}Hg]Hg^{2+}$ and the $^{197m/g}Hg^{2+}$-complexes diluted in phosphate-buffered saline (PBS) (5 μL; 1 : 1 *v/v* dilution) to assess their electrophoretic mobility.

Log $D_{7.4}$ measurements of [$^{197m/g}$Hg]Hg-NS$_4$-Tz

Aliquots of each $^{197m/g}$Hg^{2+} radiolabeled bioconjugate (10 μL) were added to a biphasic mixture of *n*-octanol (700 μL) and phosphate-buffered saline (PBS, 690 μL, pH 7.4). The mixture was vortexed for 2 min at ambient temperature and then separated *via* centrifugation (10 min, 3000 rpm). Aliquots of *n*-octanol (100 μL) and PBS (100 μL) were collected, and the activity in each portion was determined *via* gamma spectroscopy. Log $D_{7.4}$ is defined as log$_{10}$[(activity in *n*-octanol phase)/(activity in buffer phase)].

Cell binding studies with [$^{197m/g}$Hg]Hg-NS$_4$-Tz-TmAb

The HER2 binding properties of [$^{197m/g}$Hg]Hg-NS$_4$-Tz-TmAb were assessed in a direct radioligand cell-binding assay. 1 × 10^6 SK-BR-3 (HER2/neu expressing) cells suspended in phosphate buffered saline (PBS), pH 7.4 in 1.5 mL Microtubes (Diamed Lab Supplies, Mississauga, ON, Canada) were incubated with 40 nM concentrations of [$^{197m/g}$Hg]Hg-NS$_4$-TmAb in PBS, pH 7.4 in the absence or presence of a 100-fold molar excess of trastuzumab for 3.5 h at 4 °C to measure total binding (TB) and non-specific binding (NSB), respectively. The tubes were mixed by gentle agitation every 30 min to minimize adsorption of [$^{197m/g}$Hg]Hg-NS$_4$-Tz-TmAb onto the walls of the tubes. The tubes were centrifuged at 2000 rpm (400*g*) for 5 min (Eppendorf Centrifuge Model 5424, Thermo Fisher Scientific), and the supernatant was collected. Cell pellets were then rinsed with PBS and centrifuged again to collect the supernatant. This procedure was repeated once more. Once the supernatant from all rinses and the cell pellet was isolated. The cell pellets were measured in a γ-counter. NSB was subtracted from TB to obtain specific binding (SB).

In vivo studies

All animal studies were conducted in compliance with the guidelines set by the Canadian Council on Animal Care (CCAC) and approved by the Animal Care Committee (ACC) at the University of British Columbia (A20-0132 and A20-0113).

SKOV-3 xenograft mouse model. Female nude mice (8 weeks old) obtained from Jackson laboratory (JAX) were subcutaneously injected with 8 × 10^6 SKOV-3 cells in Matrigel (BD Bioscience, 1 : 1 PBS : matrigel) on the shoulder. *In vivo* imaging and biodistribution studies were performed after tumour growth reached ~8–10 mm in diameter.

Tracer preparation for *in vivo* studies with [$^{197m/g}$Hg]Hg-NS$_4$-Tz. To a solution of **NS$_4$-Tz** (0.2–0.4 μmol in 20–40 μL DMSO) in ammonium acetate (1 M, pH 7, 149–198 μL) was added to [$^{197m/g}$Hg]HgCl$_2$ (11.49–26.1 MBq in 31–61 μL 0.1 N HCl), 6 M NaOH was added (38–74 μL) to achieve a final reaction pH of 7.5. The reaction mixture was allowed to stand for 1 h at 37 °C, and the non-isolated %RCY was confirmed to be >99% *via* the iTLC methods mentioned above. The labeled tracer was diluted with PBS Tween-20 (0.01 M sodium phosphate, 0.15 M NaCl, 0.05% Tween-20) 2 : 1 (*v/v*) tracer-to-PBS for imaging doses and 1 : 2 (*v/v*) tracer-to-PBS for *ex vivo* biodistribution doses. The tracers were prepared immediately before injection

to avoid radiolysis and minimize the tracer loss to any surfaces due to its lipophilicity.

***In vivo* imaging and biodistribution of [$^{197m/g}$Hg]Hg-NS$_4$-Tz.** A total of eight healthy male C57BL/6 mice weighing approximately 29 g were divided into two groups (2 h and 4 h sacrifice times, *n* = 4 each time point), both groups received [$^{197m/g}$Hg] Hg-NS$_4$-Tz (150 μL; 3.6–5.0 MBq ^{197g}Hg for imaging, 1.5–2.0 MBq ^{197g}Hg for biodistribution) *via* tail vein injection. In each group, only one of the animals was allocated for imaging purposes, while the rest were designated for biodistribution analysis. The mice assigned for SPECT imaging were anesthetized using isoflurane *via* a precision vaporizer. To initiate anesthesia, a mixture of 5% isoflurane in oxygen was used. While for maintenance, isoflurane levels ranging from 1.5% and 2.5% in oxygen were administered. Following the induction of anesthesia, tracer was administered and subsequently whole-body images were obtained using a VECTor/CT multimodal preclinical scanner (MILabs, Utrecht, The Netherlands). The scanner was equipped with an extra-ultra high-sensitivity collimator (XUHS) 2 mm-pinhole collimator. SPECT/CT images were acquired in list mode with a dynamic scan duration of 120 min (6 frames × 20 min) for group 1, and static scans at 4 h for group 2, both were followed by a cone-beam CT scan (55 kV, 615 μA) for anatomical reference and attenuation correction. During the scanning process, the mice were kept under isoflurane anesthesia and maintained at a constant body temperature using a heating pad. The animal projection data were reconstructed using the ^{197g}Hg (energy window settings: 77 keV, 40% energy window width) according to our previously reported methods.[26] At the end of the imaging study, mice were euthanized *via* an overdose of isoflurane and treated as the biodistribution animals below.

Mice allocated for *ex vivo* biodistribution studies were administered tracer using a Tailveiner restrainer and subsequently allowed unrestricted movement within their cages. Biodistribution studies were conducted 2 hours and 4 hours after administration. To humanely euthanize the mice, ISO/ CO$_2$ asphyxiation was employed. Activity within the blood pool was retrieved *via* cardiac puncture. The organs of interest were fully extracted, weighed, and subjected to activity measurement using a gamma counter with the 55–93 keV energy window (Packard Cobra II, PerkinElmer, Waltham, MA, USA). Activity was decay corrected to time of injection. The results are reported as the percentage of the injected dose per gram of tissue (%ID/g) and the percentage of the injected dose per whole organ (%ID/organ).

Tracer preparation for *in vivo* studies with RIC [$^{197m/g}$Hg]Hg-NS$_4$-Tz-TmAb (*via* 2-step labeling). To a solution of **NS$_4$-Tz** in DMSO (10^{-3} M, 20 eq. in relation to TmAb, 158 μL) in NH$_4$OAc (1 M, pH 7, 317 μL), [$^{197m/g}$Hg]HgCl$_2$ (43.5 MBq, 60 μL) and NaOH (6 M, 80 μL) was added simultaneously. The reaction was incubated at 37 °C for 60 min, and completion (RCY >99%) was confirmed by iTLC (*via* methods mentioned above). To this labeled **NS$_4$-Tz** reaction mixture, TmAb-PEG$_4$-TCO (96.35 mg mL^{-1}, 12.2 μL in PBS, 1 eq.) was added slowly (2 μL s^{-1}). The resulting solution was sonicated for 1 min and incu-

bated at 25 °C in a thermoshaker at 500 rpm for 1 h. Purification to remove unclicked chelate was carried out by spin filtration (Amicon ultra-0.5, 50k) at 14 000g for 5 min. The filter was washed with PBS (0.4 mL, pH 7.4) (×6). The labeled tracer was collected in 224.5 μL of PBS, resulting in 15.99 MBq and 1215 μg of modified TmAb.

In vivo **imaging and biodistribution of RIC [$^{197m/g}$Hg]Hg-NS$_4$-Tz-TmAb.** Female nude mice bearing SKOV-3 xenografts were anesthetized using 5% isoflurane in oxygen in an induction chamber and restrained in a tail vein restrainer (Braintree Scientific) while under a continuous stream of 1.5–2.5% isoflurane. Mice were administered with [$^{197m/g}$Hg]Hg-NS$_4$-Tz-TmAb (2.2–2.5 MBq, 167–190 μg) (unblocked) or [$^{197m/g}$Hg]Hg-NS$_4$-Tz-TmAb (2.3–2.4 MBq, 174–182 μg) + unlabeled TmAb (1288 μg) (blocked) *via* the lateral tail vein.

Mice allocated for imaging were imaged at 4, 24, 48, and 96 h post administration (p.i.). Prior to image acquisition, mice were anesthetized *via* inhalation of 2% isoflurane-oxygen gas mixture and placed on the scanner bed with a heating pad to maintain body temperature. ^{197g}Hg SPECT/CT images were acquired and reconstructed using the same scanner and configurations as described above for the [$^{197m/g}$Hg]Hg-NS$_4$-Tz imaging studies. At the end of the last imaging time point, mice were euthanized and treated as per the *ex vivo* biodistribution studies below.

Mice allocated for *ex vivo* biodistribution studies were administered tracer using a Tailveiner restrainer and subsequently allowed unrestricted movement within their cages.

Biodistribution studies were conducted 96 hours after administration. Animals were treated analogously to the biodistribution studies above for [$^{197m/g}$Hg]Hg-NS$_4$-Tz.

Results and discussion

Synthesis and characterization of NS$_4$ BFCs

Synthesis of both bifunctional chelators started with the NS$_4$-CA precursor, synthesized using our previously reported procedures.[10] For the **NS$_4$-Tz** and **NS$_4$-NCS** derivatives, NS$_4$-CA first underwent a peptide coupling reaction with methyltetrazine-amine hydrochloride or 4-(Boc-amino)benzylamine (to yield NS$_4$-NH-Boc), respectively, followed by purification *via* HPLC (Fig. 2). This concluded the synthesis of the **NS$_4$-Tz** derivative highlighting its ease in preparation. It should be noted that the *N*-(4-(1,2,4,5-tetrazin-3-yl)benzyl)-2-(1,4,7,10-tetrathia-13-azacyclopentadecan-13-yl)acetamide (**NS$_4$-Tz-H**) derivative was also synthesized *via* peptide coupling with NS$_4$-CA and benzy-lamino tetrazine hydrochloride (Fig. 2), the non-methylated tetrazine derivatives are known to have faster kinetics in its (IEDDA) cycloaddition reaction. Compared to the methylated counterpart, the **NS$_4$-Tz-H** derivative was observed to be highly unstable upon HPLC purification. As a result, **NS$_4$-Tz-H** was not further pursued as the methylated tetrazine kinetic rates in the literature are appropriately fast enough for radiopharmaceutical applications.[27]

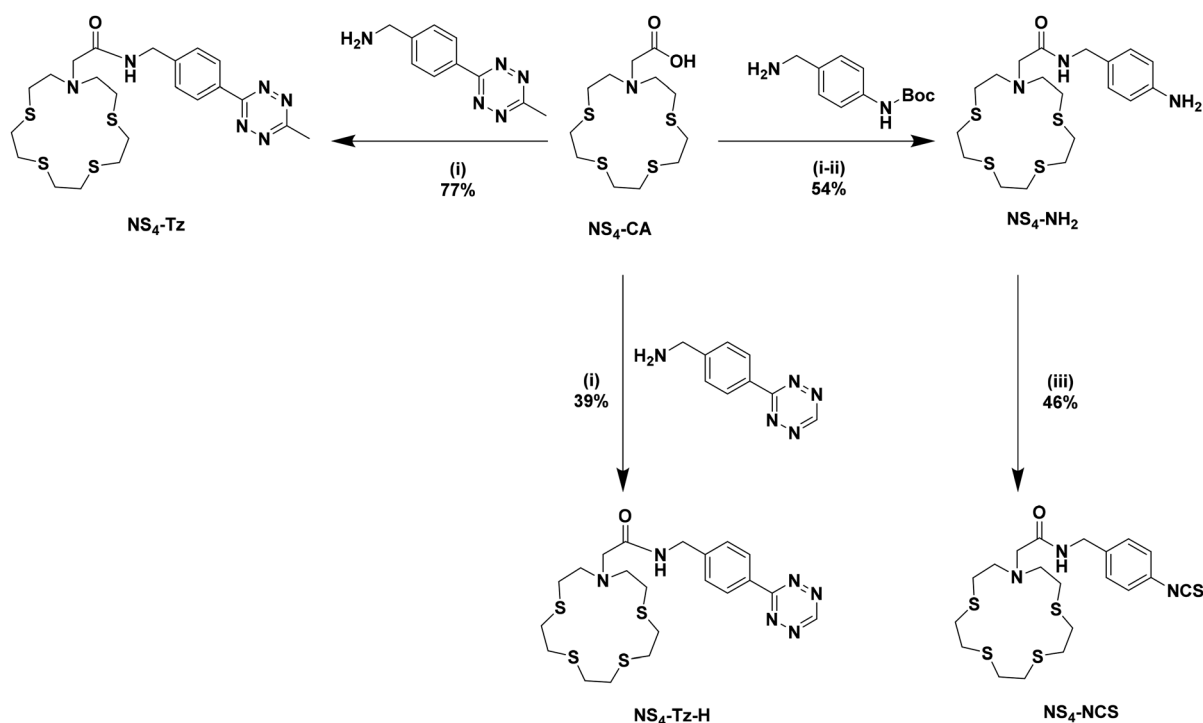Following the purification of the NS$_4$-NH-Boc, fractions were collected and HCl was added to induce Boc deprotection,

Fig. 2 Synthesis of **NS$_4$-Tz**, **NS$_4$-Tz-H** and **NS$_4$-NCS**. Reagents and conditions: (i) DMF, HATU, DIPEA, RT, Ar, overnight; (ii) ~10% 12 M HCl solution; (iii) anhydrous CH$_2$Cl$_2$, CS$_2$, TEA, acetyl chloride, Ar, 30 min, RT.

yielding **NS$_4$-NH$_2$**, which was then converted to the **NS$_4$-NCS** by adding carbon disulfide and acetyl chloride under basic conditions, following previously reported protocols.[21] The **NS$_4$-NCS** was purified by HPLC and used in radiolabeling or bioconjugation reactions within 24–48 h after isolation to avoid degradation of the Bn-NCS. This is a disadvantage to the **NS$_4$-NCS** derivative as its storage shelf-life is short compared to the NS$_4$-Tz, which remained stable at −20 °C for over 1.5 years. Additionally, the **NS$_4$-Tz** gave a higher overall synthetic yield of 77% compared to the 25% for **NS$_4$-NCS** (starting from the NS$_4$-CA), demonstrating the appeal of the **NS$_4$-Tz** BFC. All ligands and intermediates were characterized by NMR (reported in Fig. S1–S10) and Mass Spectrometry (MS).

Bifunctional chelator-trastuzumab conjugation

Following successful synthesis of the NS$_4$ BFCs, conjugation to trastuzumab (TmAb) was performed. **NS$_4$-NCS** was directly conjugated to lysine residues on TmAb *via* isothiocyanate chemistry, forming thiourea bonds (Fig. 3). The reaction, carried out with 40 equivalents of **NS$_4$-NCS** at 25 °C for 1 h at pH 8.5, yielded an average of 1.1 **NS$_4$-NCS** units per antibody (MALDI-ToF MS/MS) with a 44% recovery yield.

For tetrazine conjugation, TmAb was first modified with TCO-PEG4-NHS ester. The 4-chain polyethylene glycol derivative was used to improve solubility of the rather lipophilic **NS$_4$-Tz** and enhance the IEDDA reaction by reducing steric hindrance. PEG linkers are also known to facilitate faster blood clearance.[28] Conjugation with 8 equivalents of the TCO-PEG4-NHS ester at 25 °C, pH 9 for 1 h yielded TmAb-PEG4-TCO with 4.1 ± 0.5 TCO units per antibody (*n* = 3, MALDI-ToF MS/MS).

Subsequently, *in vitro* click reactions with TmAb-PEG4-TCO were conducted using between 10–70 equivalents of **NS$_4$-Tz** for 1 h at 25 °C (Fig. 3 and Table S1). Due to the chelator's lipophilicity, optimization was necessary to prevent antibody aggregation. Parameters such as antibody and DMSO concentration, and ligand ratios were screened (Table S1). Optimal conditions – 30 equivalents of **NS$_4$-Tz** per antibody (or 10 per TCO) – produced 3.0 **NS$_4$-Tz** units per antibody with 44% recovery (MALDI-ToF MS/MS). This level of labeling is not expected to significantly affect immunoreactivity, consistent with prior reports.[29]

[$^{197m/g}$Hg]Hg^{2+} radiolabeling with BFCs and *in vitro* stability of radiometal-complexes

[$^{197m/g}$Hg]Hg^{2+} radiolabeling with the sulfur-rich bifunctional derivatives (**NS$_4$-Tz** and **NS$_4$-NCS**) were conducted under previously established conditions for non-bifunctional **NS$_4$-BA** (37 °C, 1 h, pH 7, 1 M NH$_4$OAc; Fig. 4),[10] enabling assessment of the bifunctional arm's impact on labeling efficiency. **NS$_4$-Tz** showed excellent radiometal incorporation at 10^{-4} and 10^{-5} M (~1 MBq $^{197m/g}$Hg), with non-isolated radiochemical yields (RCYs) of >99% and 94 ± 2%, comparable to **NS$_4$-BA**. At lower ligand concentrations (10^{-6} and 10^{-7} M), **NS$_4$-Tz** RCY outperformed **NS$_4$-BA**, yielding 87 ± 1% and 13 ± 4%, respectively (compared to 34 ± 2, and 0%, respectively, for **NS$_4$-BA**).

Labeling of NS$_4$-NCS was more challenging due to non-specific interactions between [$^{197m/g}$Hg]Hg^{2+} and the isothiocyanate group, a phenomenon previously noted for DOTAM-based NCS derivatives.[6] Although the NS$_4$ scaffold has high affinity for Hg^{2+}, distinguishing Hg-incorporation into the
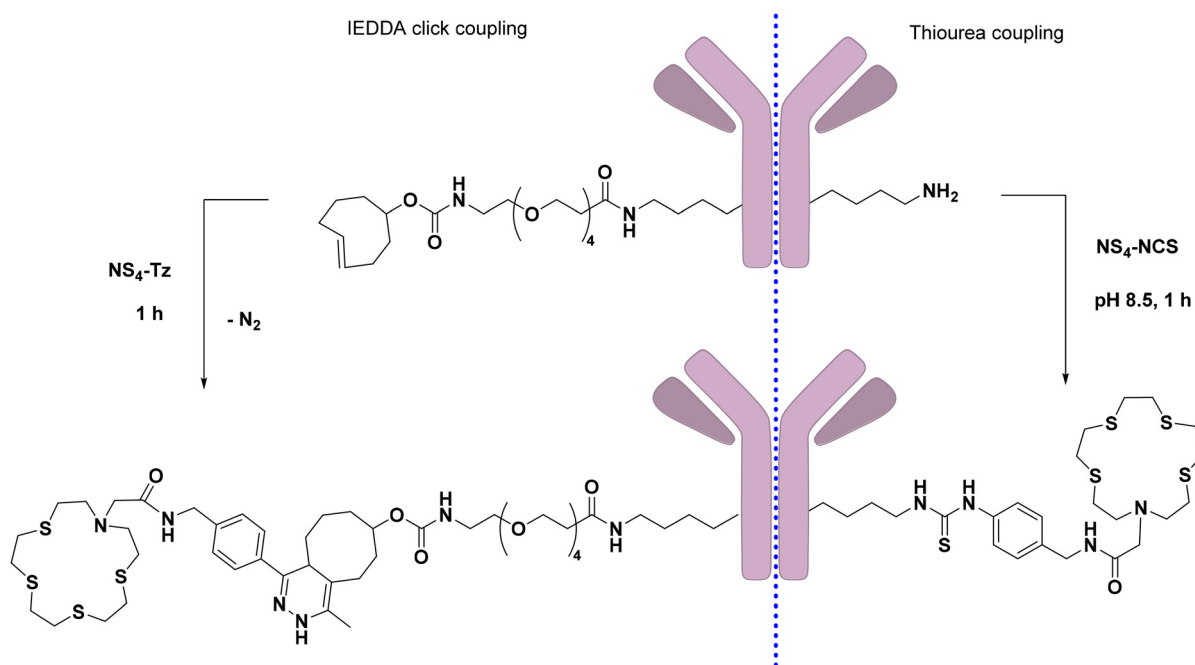

Fig. 3 Bioconjugation reactions: (right) thiourea coupling of **NS$_4$-NCS** with Trastuzumab, or (left) coupling of **NS$_4$-Tz** to PEG$_4$-TCO-modified Trastuzumab *via* the inverse electron demand Diels−Alder (IEDDA) click reaction.
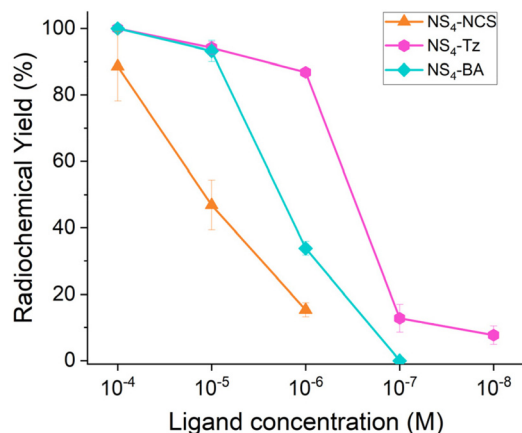
Fig. 4 Non-isolated radiochemical yields (RCYs) for [$^{197m/g}$Hg]HgCl$_2$ (~1 MBq) radiolabeling of **NS$_4$-Tz** and **NS$_4$-NCS** and **NS$_4$-BA** (1 M NH$_4$OAc, pH 7), at various ligand concentrations at 37 °C (1 h reaction time, 100 µL reaction, n = 3). [$^{197m/g}$Hg]Hg-NS$_4$-BA 80 °C labeling data is reproduced from Randhawa et al.[10]

macrocycle from NCS binding is difficult, and both likely occur. RCYs for **NS$_4$-NCS** were inferior to both the unfunctionalized macrocycle and **NS$_4$-Tz** at all ligand concentrations: 87 ± 11% (10^{-4} M), 47 ± 8% (10^{-5} M), and 15 ± 2% (10^{-6} M).

The in vitro kinetic inertness of the [$^{197m/g}$Hg]Hg-NS$_4$-Tz and [$^{197m/g}$Hg]Hg-NS$_4$-NCS was evaluated in human serum and L-glutathione (GSH) and compared to [$^{197m/g}$Hg]Hg-NS$_4$-BA (Fig. 5). Complexes were incubated in human serum at 37 °C for 137 h and analyzed via SDS-PAGE, using previously established procedures.[6,10] [$^{197m/g}$Hg]Hg-NS$_4$-Tz remained 88 ± 11% intact at 1 h, decreasing to 76 ± 1% at 15 h and stabilizing at 71 ± 6% by 137 h. [$^{197m/g}$Hg]Hg-NS$_4$-NCS showed a greater initial decline (75 ± 1% to 61 ± 8%) but also plateaued, ending with 62 ± 2% intact complex at 137 h [$^{197m/g}$Hg]Hg-NS$_4$-Tz demonstrated similar inertness to the **NS$_4$-BA** complex (72 ± 1% vs. 74 ± 7% at 24 h).

Stability against GSH (2.12 mM, 37 °C) was assessed via radio-TLC over 137 h.[25] [$^{197m/g}$Hg]Hg-NS$_4$-Tz remained >95% intact throughout. In contrast, [$^{197m/g}$Hg]Hg-NS$_4$-NCS showed an early decline, plateauing at 62 ± 6%, inferior to the **NS$_4$-BA** complex (92 ± 1% over 72 h).

The initial loss of intact [$^{197m/g}$Hg]Hg-NS$_4$-NCS in both assays suggests non-specific binding via the isothiocyanate, with rapid transchelation of NCS-bound Hg^{2+} and stable retention of macrocycle-bound metal. Alternatively, the reduced stability of [$^{197m/g}$Hg]Hg-NS$_4$-NCS relative to the previously studied [$^{197m/g}$Hg]Hg-NS$_4$-BA analogue may arise from intrinsic differences between the p-SCN-Bn substituent in the former and the benzyl group in the latter. Our prior computational studies suggest that the benzyl substituent could stabilise the Hg^{2+} complex through a π-cation interaction.[10] As such, this stabilizing effect would be expected to vary depending on the electronic properties of the substituents on the benzyl ring (electron-donating versus electron-withdrawing). However, experimental and computations studies are required to confirm this hypothesis. Nonetheless, due to its lower stability and labeling specificity, **NS$_4$-NCS** was excluded from further study, while **NS$_4$-Tz** was advanced to further in vitro and in vivo studies.

[$^{197m/g}$Hg]Hg^{2+} radiolabeling, stability and immunoreactivity of immunoconjugates

Following successful radiolabeling of the BFCs, the **NS$_4$-Tz** immunoconjugate (NS$_4$-Tz-TmAb, vide supra) was radiolabeled with [$^{197m/g}$Hg]Hg^{2+} and evaluated in vitro. Initial labeling (4.6 MBq, 150 µg) yielded a pre-purification RCY of 47 ± 17%. Interestingly, radiolabeling of the unmodified TmAb yielded a comparable labeling yield (48 ± 10%) under analogous conditions, indicating significant non-specific binding – likely to thiol-containing amino acid residues such as cysteine. Purification of the radiolabeled unmodified and chelator-conjugated TmAb using spin desalting columns and 50 kDa spin
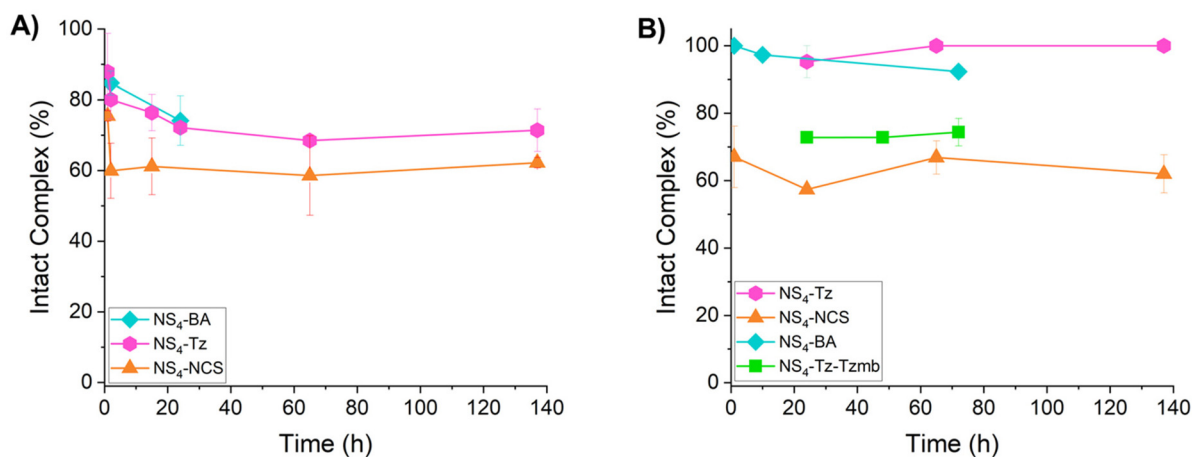

Fig. 5 Kinetic inertness of [$^{197m/g}$Hg]Hg-NS$_4$-Tz, [$^{197m/g}$Hg]Hg-**NS$_4$-NCS** and [$^{197m/g}$Hg]Hg-NS$_4$-Tz-TmAb against (A) human serum (excluding [$^{197m/g}$Hg]Hg-NS$_4$-Tz-TmAb) and (B) glutathione with comparison to the formally reported **NS$_4$-BA** [$^{197m/g}$Hg]Hg-NS$_4$-BA stability data is reproduced from Randhawa et al.[10]
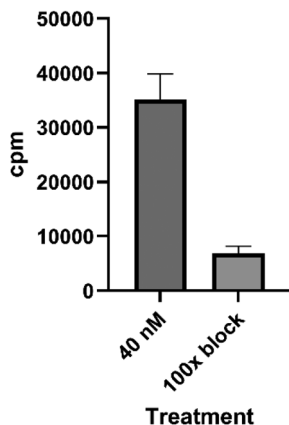
Fig. 6 One-point cell binding assay in SK-BR-3 cells treated with [$^{197m/g}$Hg]Hg-NS$_4$-Tz-TmAb (40 nM) or with the addition of 100× unlabeled TmAb.
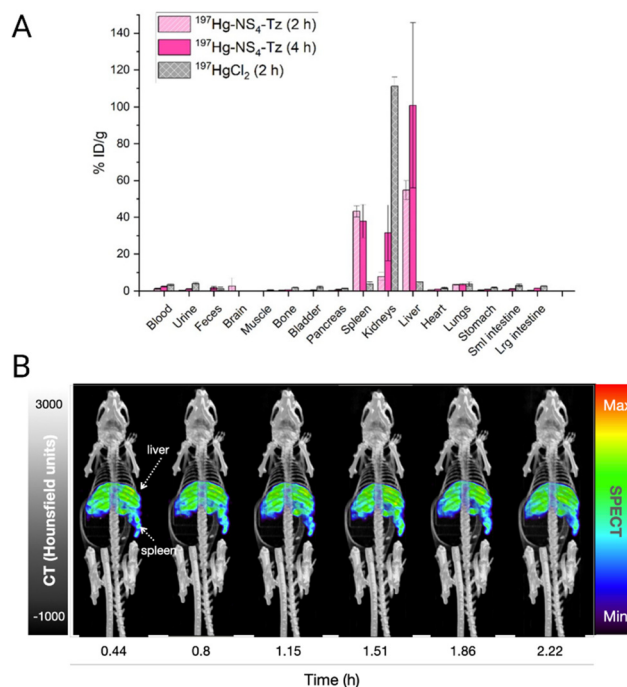

Fig. 7 (A) Biodistribution results of [^{197g}Hg]Hg-NS$_4$-Tz in healthy male C57BL/6 mice after 2 and 4 h post-administration ($n = 4$, per time point), with comparison to the biodistribution of [^{197g}Hg]HgCl$_2$ at 2 h post-administration represented as percent injected dose per gram of tissue (%ID/g). [^{197g}Hg]HgCl$_2$ biodistribution data is reproduced from Randhawa et al.;[26] (B) SPECT/CT images depicting frontal view from a total body SPECT/CT scan obtained 0–2 hours following administration of [$^{197m/g}$Hg]Hg-NS$_4$-Tz. Images reconstructed using the 77 keV photopeak.

filters was conducted, resulting in radiochemical purities (RCPs) of 33 ± 8% for [$^{197m/g}$Hg]Hg-TmAb (without chelator) and 39 ± 5% for the **NS$_4$-Tz** immunoconjugate, as determined by radio-TLC. However, SDS-PAGE confirmed no 'free' [$^{197m/g}$Hg]Hg^{2+} remained, suggesting true RCP was >99% (Fig. S12). The discrepancy with iTLC is likely attributed to DMSA (50 mM) used in the mobile phase, which may transchelate the non-specifically weakly bound Hg^{2+}, leading to false negatives, while chelator-bound Hg^{2+} remains intact, as previously demonstrated for the BFCs.

To avoid non-specific labeling, a two-step labeling approach was used: [$^{197m/g}$Hg]Hg^{2+} was first quantitatively complexed with **NS$_4$-Tz** (RCY >99%), then conjugated to TCO-PEG4-TmAb. SDS-PAGE and iTLC confirmed post-purification RCP of >99% (Fig. S11). Due to poor aqueous solubility of **NS$_4$-Tz** at ≥10^{-3} M, 20% DMSO was required during labeling.

The purified immunoconjugate was incubated with GSH (72 h); demetallation began at 24 h, with 74 ± 4% intact complex remaining at 72 h (Fig. 5B). Serum stability was not quantified due to co-migration of labeled antibody and Hg-bound serum proteins on SDS-PAGE (Fig. S14).

To verify HER2 targeting, a one-point binding assay was performed in HER2/neu-overexpressing SK-BR-3 cells. Binding of [$^{197m/g}$Hg]Hg-NS$_4$-Tz-TmAb was competitively inhibited by 100-fold excess unlabeled TmAb, confirming retained immunoreactivity and specific HER2 binding (Fig. 6).

In vivo SPECT/CT imaging and ex vivo biodistribution of [$^{197m/g}$Hg]Hg-NS$_4$-Tz

The encouraging radiolabeling efficiency and stability of **NS$_4$-Tz** prompted further evaluation of its in vivo behaviour. The pharmacokinetics and biodistribution of [$^{197m/g}$Hg]Hg-NS$_4$-Tz were assessed through ex vivo biodistribution at 2 and 4 h, and dynamic in vivo SPECT/CT imaging over 2 h, analysed using the ^{197g}Hg photon energy windows, as previously described.[26] Results were compared to the those of unchelated ^{197g}HgCl$_2$[26] (Fig. 7 and Fig. S15, S16, Tables S2, S3).

At 2 hours post-injection, unchelated ^{197g}HgCl$_2$ showed predominant accumulation in the cortex of the kidney (111 ± 5% ID/g), consistent with prolonged renal retention. In contrast, ^{197g}Hg-NS$_4$-Tz exhibited highest uptake in the liver (54.75 ± 5.16% ID/g) and spleen (43.21 ± 3.08% ID/g), with moderate accumulation in the kidneys (7.94 ± 2.14% ID/g). This distribution pattern aligns with the tracer's high lipophilicity (log $D_{7.4}$ = 1.2 ± 0.09, determined by the "shake-flask" method), which favors uptake by the reticuloendothelial system (RES).

By 4 hours, splenic uptake of ^{197g}Hg-NS$_4$-Tz remained relatively stable (37.83 ± 9.06% ID/g), while liver and kidney accumulation increased to 100.85 ± 44.88% ID/g and 31.48 ± 15.11% ID/g, respectively. These findings suggest clearance of the tracer primarily via RES rather than renal accumulation, in contrast to unchelated ^{197g}Hg.

Moderate kidney uptake at 2 hours may suggest in vivo stability of the tracer over this period, indicating minimal or moderate release of free mercury into circulation. This conclusion is further supported by in vitro serum and GSH stability studies (Fig. 5A and B), which showed no significant transmetalation over 137 hours. However, the ~23% increase in renal uptake between 2 and 4 hours complicates the interpretation of longer-term in vivo stability. This may reflect delayed renal excretion of the tracer or gradual transchelation in vivo.

***In vivo* SPECT/CT imaging and *ex vivo* biodistribution of [$^{197m/g}$Hg]Hg-NS$_4$-Tz-TmAb**

Finally, the *in vivo* behaviour of the immunoconjugate [^{197}Hg]Hg-NS$_4$-Tz-TmAb was assessed in SKOV-3 tumour-bearing mice

over 96 hours, unblocked ($n = 4$) and blocking studies ($n = 2$) were conducted (Fig. 8 and Table S4). The radioimmunoconjugate was prepared *via* the 2-step labeling approach described above to eliminate non-specifically bound Hg^{2+}. The *ex vivo* biodistribution results at 96 hours showed highest accumu-
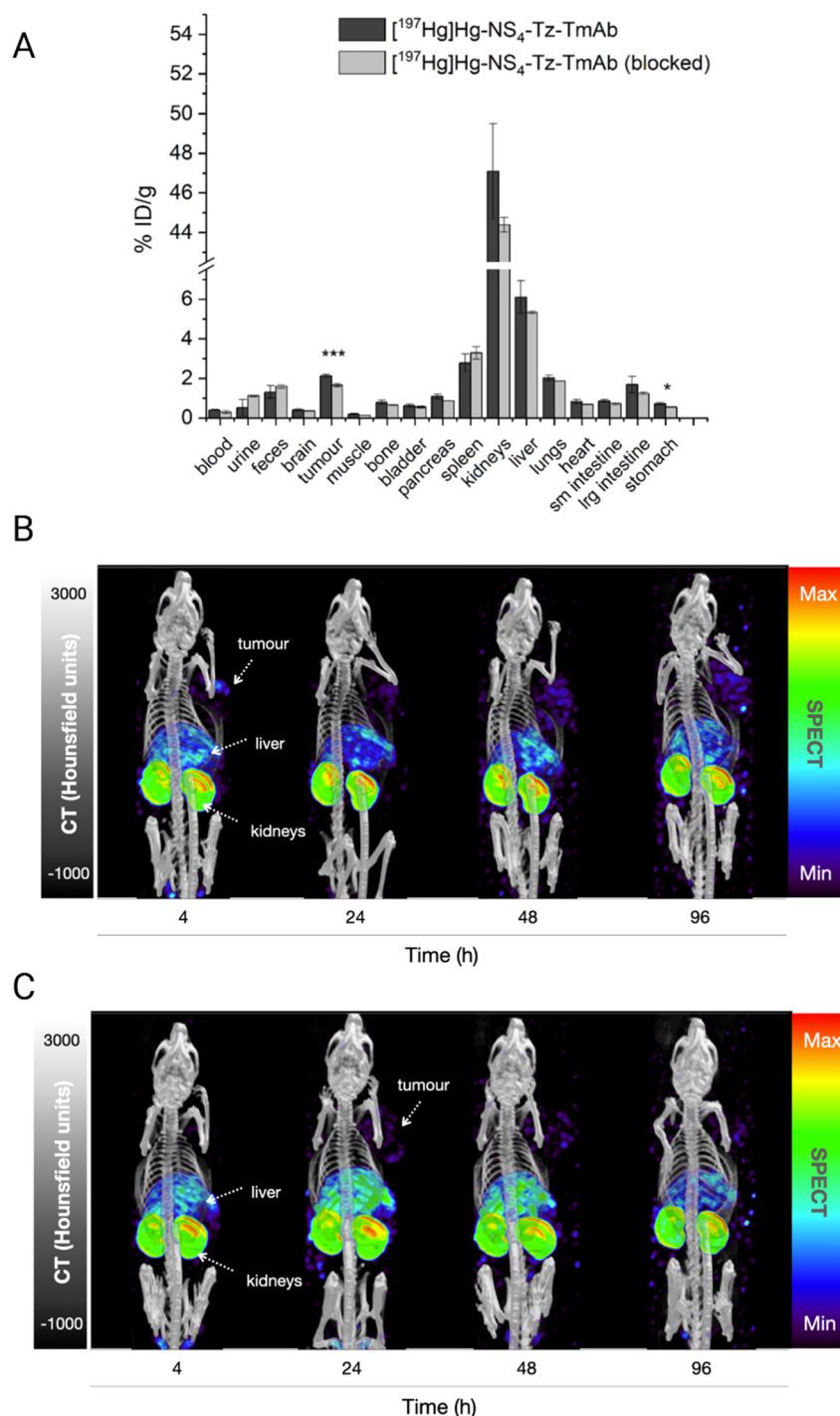
Fig. 8 (A) Biodistribution results 4 days post administration of [^{197}Hg]Hg-NS$_4$-Tz-TmAb in mice bearing SKOV3 tumour xenografts, unblocked ($n = 4$) and blocked ($n = 2$) represented as percentage of injected dose per gram of tissue (%ID/g). Unpaired *t*-test comparing unblocked and blocked uptake: $p < 0.05$ = *; $p < 0.01$ = **; $p < 0.001$ = ***; and SPECT/CT images depicting frontal view from a total body SPECT/CT scan obtained 0–96 hours following administration of [$^{197m/g}$Hg]Hg-NS$_4$-Tz-TmAb in nude mice bearing SKOV-3 xenograft; (B) unblocked, (C) blocked. Images reconstructed using the 77 keV photopeak.

lation of the tracer in the kidneys (47.10 ± 2.39% ID/g), with residual uptake in the liver (6.11 ± 0.83% ID/g), spleen (2.78 ± 0.46% ID/g), and tumour (2.13 ± 0.08% ID/g). While residual liver and spleen uptake is common for radioimmunoconjugates, the high kidney uptake is characteristic of unchelated ^{197}Hg, suggesting significant transmetalation *in vivo*. Nonetheless, blocking studies with co-injection of excess unlabeled trastuzumab, showed specific blocking and reduction of uptake in SKOV-3 tumours (1.65 ± 0.09% ID/g), compared to non-blocking studies ($p < 0.001$). Uptake in all other organs was not statistically different, except the stomach (0.73 ± 0.07 *vs.* 0.55 ± 0.02% ID/g, for unblocked and blocked experiments, respectively; $p < 0.05$). Qualitative SPECT/CT imaging was able to visualize tumour uptake as early as 4 hours in the non-blocking animal group, with minimal uptake at the same time point for the blocking studies.

Despite the lower-than-expected tumour uptake, blocking experiments validated receptor mediated uptake of [^{197}Hg]Hg-NS$_4$-Tz-TmAb, to our knowledge this is the first report of targeted delivery of the $^{197m/g}$Hg theranostic pair using a radioimmunoconjugate. Off-target kidney uptake of the radiotracer suggests that the $^{197m/g}$Hg-NS$_4$ complex conjugated to TmAb may suffer from instability *in vivo*, this lability was also observed to some degree in the *in vitro* stability challenge assay in GSH (*vide supra*). These results suggest there may exist competitive binding between specific (chelator)-bound Hg^{2+} and non-specific (amino acid residue)-bound Hg^{2+} on the immunoconjugate, and/or the stability of the Hg-NS$_4$-Tz complex is altered upon coupling of the Tz-handle to the TCO-modified antibody. Modification of the linker and alternate bioconjugation strategies, to improve the kinetic inertness of the complex and also the pharmacodynamics of the rather lipophilic BFC are warranted to further investigate the NS$_4$ scaffold as a chelator for the delivery of $^{197m/g}$Hg *in vivo*.

Conclusion

Two novel [$^{197m/g}$Hg]Hg^{2+} bifunctional chelators (BFCs) **NS$_4$-Tz** and **NS$_4$-NCS** were designed for bioconjugation to targeting vectors based on the previous success of non-functionalized **NS$_4$-BA**. Radiolabeling and complex stability of **NS$_4$-Tz** with [$^{197m/g}$Hg]Hg^{2+} resulted in a comparable yield to **NS$_4$-BA**, quantitatively complexing [$^{197m/g}$Hg]Hg^{2+} in 60 min at 37 °C with high *in vitro* stability against GSH and human serum, remaining >95% intact and 71 ± 6% intact over 137 h, respectively. However, **NS$_4$-NCS** resulted in a decreased RCY and exhibited kinetic lability compared to the former; non-specific Hg^{2+} binding to the NCS group may contribute to this instability. Both NS$_4$ BFCs were successfully conjugated to trastuzumab (TmAb), an antibody targeting the HER2 receptor overexpressed in many breast and ovarian cancers. The NS$_4$-Tz-TmAb conjugate yielded an appropriate number of chelators per antibody (3 chelators per mAb), while NS$_4$-NCS-TmAb click yield was too low (1.1 chelators per mAb) for future applications. Subsequently, NS$_4$-Tz-TmAb radiolabeling, purifi-

cation and isolation were investigated. Of note, a high degree of nonspecific binding of [$^{197m/g}$Hg]Hg^{2+} to the antibody was observed. To avoid unstable non-specific binding to TmAb, the two-step "*in vivo*" click labeling with [$^{197m/g}$Hg]Hg-NS$_4$-Tz was employed for further stability and cell assays. The two-step radiolabeled immunoconjugate [$^{197m/g}$Hg]Hg-NS$_4$-Tz-TmAb displayed a slight reduction in the kinetic stability of the tracer against GSH compared to that of the [$^{197m/g}$Hg]Hg-NS$_4$-Tz complex alone. To determine the **NS$_4$-Tz** viability in further *in vivo* applications the stability, pharmacokinetics, and biodistribution of the [$^{197m/g}$Hg]Hg-NS$_4$-Tz tracer was assessed *via* *ex vivo* biodistribution and *in vivo* SPECT/CT imaging over 4 h. The lipophilic radiotracer demonstrated high uptake in the liver and spleen over 4 h. However, increased kidney uptake could also be seen over the 2 h to 4 h experiments; it is unclear whether this is a result of transchelation of the tracer *in vivo* over time or the tracer pharmacokinetics.

Finally, the first targeted *in vivo* study with [$^{197m/g}$Hg]Hg-NS$_4$-Tz-TmAb was conducted. Although high kidney uptake at 4 days post administration was observed, indicating transmetalation of ^{197}Hg over time, blocking studies confirmed specific uptake of [$^{197m/g}$Hg]Hg-NS$_4$-Tz-TmAb to SKOV-3 tumours in mice. To our knowledge, this is the first time targeted delivery of a ^{197}Hg-labeled immunoconjugate is presented.

Overall, the **NS$_4$-Tz** was proven to be a suitable BFC due to its simple synthesis, long shelf life, and high labeling and bioconjugation efficiency. While long-term *in vivo* stability of the conjugate is likely insufficient for applications with antibodies, the use of this chelator for targeting with biomolecules of shorter biological half-life (small molecules, peptides) may be warranted. Additionally, integration of hydrophilic linkers to improve water solubility and pharmacokinetics of the Hg-NS$_4$-Tz complexes should be pursued in the future.

The observation of significant non-specific [$^{197m/g}$Hg]Hg^{2+} labeling of Trastuzumab will likely complicate the application of this isomer pair with immunoconjugates. While our tetrazine-bearing chelator could circumvent this challenge by implementing a 2-step labeling strategy, this would in turn hinder clinical translation by the need for additional quality control and steps in radiopharmaceutical formulation. Testing our NS$_4$ systems when conjugated to small molecule and/or peptide biomolecules to minimize non-specific labeling, along with the continued search for new and effective chelators that will enable the use of next-generation theranostic radiopharmaceuticals with $^{197m/g}$Hg will be pursued in future studies.

Author contributions

PR: conceptualization, data curation, formal analysis, investigation, methodology, visualization, writing – original draft, review and editing. MK: investigation, writing – review and editing. AC: formal analysis, investigation, writing – review and editing. CRR: formal analysis, investigation, visualization, writing – original draft, review and editing. ZC: investigation, methodology, writing – review and editing. CC: investigation,

methodology, writing – review and editing. YG-S: investigation, methodology, writing – review and editing. SC: investigation, writing – review and editing. NW: investigation, methodology, writing – review and editing. PRWJD: formal analysis, investigation, visualization, writing – original draft, review and editing. HM: investigation, writing – review and editing. RR: resources, supervision, writing – review and editing. VR: resources, supervision, writing – review and editing. CFR: conceptualization, funding acquisition, methodology, project administration, resources, supervision, writing – original draft, review and editing.

Conflicts of interest

The authors have no conflicts of interest to declare.

Data availability

The data supporting this article have been included as part of the supplementary information (SI). Supplementary information: NMR characterization of compounds, procedures and table of results for optimization of bifunctional chelator-trastuzumab conjugation reactions, experimental procedures for non-specific $^{197m/g}$Hg labeling studies with antibodies, SDS-PAGE radiotraces, *ex vivo* biodistribution tables and graphs for [^{197}Hg]Hg-NS$_4$-Tz and [^{197}Hg]Hg-NS$_4$-Tz-TmAb. See DOI: https://doi.org/10.1039/d5pm00222b.

Acknowledgements

References

1 P. Randhawa, A. P. Olson, S. Chen, K. L. Gower-fry, C. Hoehr, J. W. Engle, C. F. Ramogida and V. Radchenko, Meitner-Auger electron emitters for targeted radionuclide therapy : Antimony-119 and mercury- 197m/g, *Curr. Radiopharm.*, 2021, **14**, 1–26.

2 A. Ku, V. J. Facca, Z. Cai and R. M. Reilly, Auger electrons for cancer therapy – a review, *EJNMMI Radiopharm. Chem.*, 2019, **4**, 27.

3 Z. Cai, N. Al-saden, C. J. Georgiou and R. M. Reilly, Cellular dosimetry of ^{197}Hg, ^{197m}Hg and ^{111}In: comparison of dose deposition and identification of the cell and nuclear membrane as important targets, *Int. J. Radiat. Biol.*, 2020, 1–22.

4 M. K. Brown, Z. Cai, C. J. Georgiou, S. Chen, Y. Ganga-Sah, V. Radchenko, J. T. Rutka and R. M. Reilly, Auger electron-emitting EGFR-targeted and non-targeted [^{197}Hg]Hg-gold nanoparticles for treatment of glioblastoma multiforme (GBM), *EJNMMI Radiopharm. Chem.*, 2025, **10**, 45.

5 R. G. Pearson, Hard and soft acids and bases. HSAB, Part 1: fundamentals principles, *J. Chem. Educ.*, 1986, **45**, 581–587.

6 P. Randhawa, I. Carbo-Bague, P. R. W. J. Davey, S. Chen, H. Merkens, C. F. Uribe, C. Zhang, M. Tosato, F. Bénard, V. Radchenko and C. F. Ramogida, Exploration of commercial cyclen-based chelators for mercury-197m/g incorporation into theranostic radiopharmaceuticals, *Front. Chem.*, 2024, **12**, 1292566.

7 M. Tosato, P. Randhawa, M. Asti, L. B. S. Hemmingsen, C. A. O'Shea, P. Thaveenrasingam, S. P. A. Sauer, S. Chen, C. Graiff, I. Menegazzo, M. Baron, V. Radchenko, C. F. Ramogida and V. Di Marco, Capturing Mercury-197m/g for Auger Electron Therapy and Cancer Theranostic with Sulfur-Containing Cyclen-Based Macrocycles, *Inorg. Chem.*, 2024, **63**, 14241–14255.

8 I. Carbo-Bague and C. F. Ramogida, *Emerging Therapeutic Radiopharmaceutical and Their Theranostic Pairs, Encyclopedia of Inorganic and Bioinorganic Chemistry*, Wiley, 2021, pp. 1–34. https://doi.org/10.1002/9781119951438.eibc2763.

9 I. M. F. Gilpin, M. Ullrich, T. Wünsche, K. Zarschler, O. Lebeda, J. Pietzsch, H. Pietzsch and M. Walther, Radiolabelled Cyclic Bisarylmercury: High Chemical and in vivo Stability for Theranostics, *ChemMedChem*, 2021, **16**, 2645–2649.

10 P. Randhawa, K. L. Gower-Fry, C. M. K. Stienstra, M. Tosato, S. Chen, Y. Gao, A. W. McDonagh, V. Di Marco, V. Radchenko, G. Schreckenbach and C. F. Ramogida, Selective Chelation of the Exotic Meitner–Auger Emitter Mercury–197m/g with Sulfur–Rich Macrocyclic Ligands: Towards the Future of Theranostic Radiopharmaceuticals, *Chem. – Eur. J.*, 2023, **29**, e202203815.

11 C. Chan, V. Prozzo, S. Aghevlian and R. M. Reilly, Formulation of a kit under Good Manufacturing Practices (GMP) for preparing [^{111}In]In-BnDTPA-trastuzumab-NLS injection: a theranostic agent for imaging and Meitner-Auger Electron (MAE) radioimmunotherapy of HER2-positive breast cancer, *EJNMMI Radiopharm. Chem.*, 2022, **7**, 33.

12 K. E. Bailey, D. L. Costantini, Z. Cai, D. A. Scollard, Z. Chen, R. M. Reilly and K. A. Vallis, Epidermal growth factor receptor inhibition modulates the nuclear localization and cytotoxicity of the Auger electron-emitting radiopharmaceutical ^{111}In-DTPA-human epidermal growth factor, *J. Nucl. Med.*, 2007, **48**, 1562–1570.

13 D. L. Costantini, K. Bateman, K. McLarty, K. A. Vallis and R. M. Reilly, Trastuzumab-resistant breast cancer cells remain sensitive to the auger electron-emitting radiotherapeutic agent ^{111}In-NLS-trastuzumab and are radiosensitized by methotrexate, *J. Nucl. Med.*, 2008, **49**, 1498–1505.

14 M. P. Kelly, F.-T. Lee, K. Tahtis, B. E. Power, F. E. Smyth, M. W. Brechbiel, P. J. Hudson and A. M. Scott, Tumor Targeting by a Multivalent Single-Chain Fv (scFv) Anti-Lewis Y Antibody Construct, *Cancer Biother. Radiopharm.*, 2008, **23**, 411–424.

15 S. M. Sarrett, O. Keinänen, E. J. Dayts, G. Dewaele-Le Roi, C. Rodriguez, K. E. Carnazza and B. M. Zeglis, Inverse electron demand Diels–Alder click chemistry for pretargeted PET imaging and radioimmunotherapy, *Nat. Protoc.*, 2021, **16**, 3348–3381.

16 A. Rondon and F. Degoul, Antibody Pretargeting Based on Bioorthogonal Click Chemistry for Cancer Imaging and Targeted Radionuclide Therapy, *Bioconjugate Chem.*, 2020, **31**, 159–173.

17 S. M. Cheal, S. K. Chung, B. A. Vaughn, N.-K. V. Cheung and S. M. Larson, Pretargeting: A Path Forward for Radioimmunotherapy, *J. Nucl. Med.*, 2022, **63**, 1302–1315.

18 S. Poty, L. Ordas, Y. Dekempeneer, A. A. Parach, L. Navarro, F. Santens, N. Dumauthioz, M. Bardiès, T. Lahoutte, M. D'Huyvetter and J.-P. Pouget, Optimizing the Therapeutic Index of sdAb-Based Radiopharmaceuticals Using Pretargeting, *J. Nucl. Med.*, 2024, **65**, 1564–1570.

19 B. M. Zeglis, K. K. Sevak, T. Reiner, P. Mohindra, S. D. Carlin, P. Zanzonico, R. Weissleder and J. S. Lewis, A Pretargeted PET Imaging Strategy Based on Bioorthogonal Diels–Alder Click Chemistry, *J. Nucl. Med.*, 2013, **54**, 1389–1396.

20 D. Bauer, M. A. Cornejo, T. T. Hoang, J. S. Lewis and B. M. Zeglis, Click Chemistry and Radiochemistry: An Update, *Bioconjugate Chem.*, 2023, **34**, 1925–1950.

21 A. W. McDonagh, B. L. McNeil, B. O. Patrick and C. F. Ramogida, Synthesis and Evaluation of Bifunctional [2.2.2]-Cryptands for Nuclear Medicine Applications, *Inorg. Chem.*, 2021, **60**, 10030–10037.

22 N. A. Thiele, V. Brown, J. M. Kelly, A. Amor-coarasa, U. Jermilova, S. N. Macmillan, A. Nikolopoulou, S. Ponnala, C. F. Ramogida, A. K. H. Robertson, C. Rodr, P. Schaffer, C. Williams, J. W. Babich, V. Radchenko and J. J. Wilson, An Eighteen-Membered Macrocyclic Ligand for Actinium-225 Targeted Alpha Therapy, *Angew. Chem., Int. Ed.*, 2017, **56**, 14712–14717.

23 S. Chen, M. Bas, S. Happel, P. Randhawa, S. McNeil, E. Kurakina, S. Zeisler, K. Maskell, C. Hoehr, C. F. Ramogida and V. Radchenko, Determination of distribution coefficients of mercury and gold on selected extraction chromatographic resins - towards an improved separation method of mercury-197 from proton-irradiated gold targets, *J. Chromatogr. A*, 2023, **1688**, 463717.

24 X. Huang and C. Zhou, Nuclear Data Sheets for A = 197, *Nucl. Data Sheets*, 2005, **104**, 283–426.

25 D. A. Dickinson and H. J. Forman, Cellular glutathione and thiols metabolism, *Biochem. Pharmacol.*, 2002, **64**, 1019–1026.

26 P. Randhawa, C. Rodríguez-Rodríguez, H. Koniar, P. R. W. J. Davey, S. Chen, V. Radchenko and C. F. Ramogida, Quantitative dual-isotope preclinical SPECT/CT imaging and biodistribution of the mercury-197m/g theranostic pair with [197m/g]Hg]HgCl$_2$ and a [197m/g]Hg]Hg-tetrathiol complex as a platform for radiopharmaceutical development, *EJNMMI Radiopharm. Chem.*, 2025, https://www.researchsquare.com/article/rs-7216255/v1, accepted.

27 J. A. Wagner, D. Mercadante, I. Nikić, E. A. Lemke and F. Gräter, Origin of Orthogonality of Strain–Promoted Click Reactions, *Chem. – Eur. J.*, 2015, **21**, 12431–12435.

28 W. Lee, K. N. Bobba, J. Y. Kim, H. Park, A. Bhise, W. Kim, K. Lee, S. Rajkumar, B. Nam, K. C. Lee, S. H. Lee, S. Ko, H. J. Lee, S. T. Jung and J. Yoo, A short PEG linker alters the *in vivo* pharmacokinetics of trastuzumab to yield high-contrast immuno-PET images, *J. Mater. Chem. B*, 2021, **9**, 2993–2997.

29 S. K. Sharma, J. M. Glaser, K. J. Edwards, E. Khozeimeh Sarbisheh, A. K. Salih, J. S. Lewis and E. W. Price, A Systematic Evaluation of Antibody Modification and [89]Zr-Radiolabeling for Optimized Immuno-PET, *Bioconjugate Chem.*, 2021, **32**, 1177–1191.